

ANTARES/VIRGO Coincidences : a feasibility study

Thierry PRADIER

*Institut Pluridisciplinaire Hubert Curien (IPHC/DRS)
& University Louis-Pasteur, Strasbourg (France)*

Sources of gravitational waves (GW) and emitters of high energy (HE) neutrinos both involve compact objects and matter moving at relativistic speeds. Coincidences between VIRGO and ANTARES would give a unique insight on the physics of the most powerful objects in the Universe. The feasibility of such GW/HE ν coincidences is analysed.

The forthcoming years should be very exciting both in GW astronomy and HE ν astronomy. The VIRGO interferometer¹, currently closed down for upgrade, should be taking data with an improved injection system in 2009, whereas the ANTARES collaboration has completed the deployment and connections of its 12 lines² early in June 2008, starting the operation of the first *undersea* neutrino telescope. The two LIGO interferometers (ITF) are in operation³, and ICECUBE is deploying its 1 km³ neutrino telescope in the ice of the South Pole, already having 40 lines in data taking mode⁴. Both GW sources and HE ν emitters involve compact objects and matter moving at relativistic speeds. As a result, time coincidences between VIRGO and ANTARES can be envisaged. Some astrophysical objects, invisible in electromagnetic channels, may be observable only *via* their GW and HE ν emissions. Finally, in many quantum gravity (QG) models⁵, the propagation velocity of a particle depends on the energy: measuring a non-zero time delay between GW bursts and HE ν transients would allow to probe QG effects.

1 GW bursters and HE ν sources : the case for microquasars major outbursts

Flares from soft-gamma repeaters⁶, core-collapse supernovae and gamma-ray bursts are commonly cited sources both for GW bursts and neutrino emissions, but are described elsewhere⁷. Microquasars are galactic jet sources associated with some classes of X-ray binaries involving both neutron stars and black hole candidates⁸. The content of jets in microquasars remains an open issue. In scenarios in which an initial rise of the X-ray flux leads to ejection of the inner part of the accretion disk, as is widely claimed to be suggested by the anticorrelation between the X-ray and radio flares seen during major ejection events, e-p jets are expected to be produced. A possible diagnostic of e-p jets is the presence of Doppler-shifted spectral lines, such as the H α line as seen in SS433. Taking the example of LS 5039, some authors argue in favor of hadronic origin of TeV photons⁹. The flux of TeV neutrinos estimated on the basis of the detected TeV γ -ray flux depends significantly on the location of γ -ray production region. The HESS/EGRET data agree well with a production of γ/ν at the base of the jet, as seen in figure 1⁹, close to the onset of the acceleration phase and its corresponding GW signal.

The matter accreted for months/years could be *swallowed* by the compact object⁷, and, provided that the process is fast, trigger the resonance of normal modes of the central object,

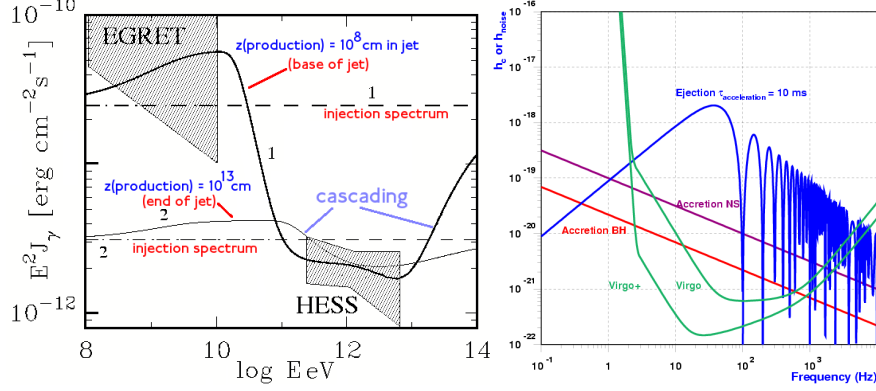


Figure 1: Left : γ Data from EGRET and HESS, together with predictions for models with production of γ at the base or at the end of the jet. Right : Amplitudes expected for the accretion/ejection processes at 1 kpc, for $\delta m \sim 10^{-4} M_{\odot}$, $\tau_{\text{acc}} \sim 10$ ms, $\gamma = 10$.

typically a damped sine signal, which could last during the ejection phase. The acceleration of an ultrarelativistic blob of matter with a Lorentz factor γ around a compact object induces a *burst with memory* independent on the density of the ejecta¹⁰. The frequency is typically the inverse of the acceleration time t_{acc} . For both signals, the amplitude will critically depend on the accreted/ejected mass, which can be estimated to range from $10^{-8} M_{\odot}$ up to $10^{-4} M_{\odot}$, for major events. A summary of these estimates for the most extreme outbursts are displayed in Figure 1.

2 Observability of ANTARES/VIRGO Coincidences

Both VIRGO and ANTARES have limited sky coverage and exposure. In order to perform coincidences between both detectors, the overlap of such visibility maps has to be computed. The response $h(t)$ of an interferometric detector to a GW is a linear combination of the two independent wave polarizations h_+ and h_{\times} , with weighting factors called the beam pattern functions. The instantaneous beam pattern (normalised to its maximal value, and averaged over the unknown polarization angle) in equatorial coordinates (right ascension α , declination δ) is displayed in figure 2 for VIRGO.

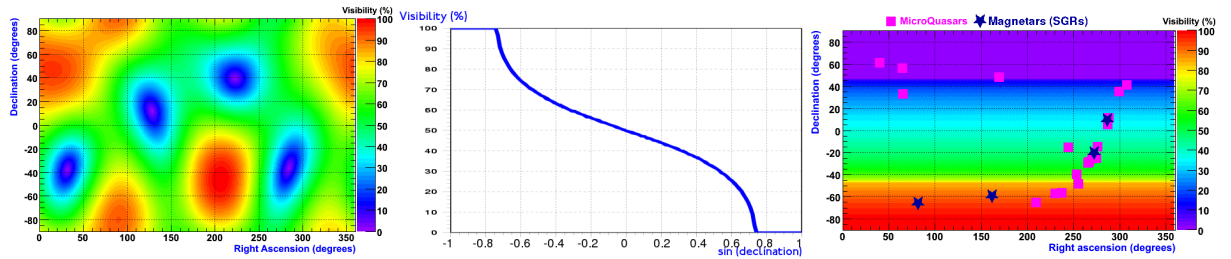


Figure 2: Left : VIRGO beam pattern in equatorial coordinates. Middle : ANTARES daily averaged visibility vs $\sin \delta$. Right : Common visibility sky map for ANTARES and VIRGO.

Searching for neutrinos which have interacted in the Earth, ANTARES is only sensitive to sources below the horizon at some time during the day. Figure 2 shows the daily average visibility as a function of $\sin \delta$. Finally, the visibility sky map for coincidences between ANTARES and VIRGO is the convolution of the two previous exposure maps. The daily averaged common sky map is displayed in figure 2, together with the position of known microquasars and soft-gamma repeaters (or magnetars). Most of these galactic sources are visible at some time by both experiments, rendering observable GW/HE ν coincidences for these sources.

3 Detectability of ANTARES/VIRGO Coincidences

To set the coincidence time window, possible physical propagation delays have to be estimated. In the case of GW, the graviton being massless, and the energy carried away by each individual graviton in a GW burst being small ($E_{\text{graviton}} \sim hf \ll 1$ for $f = 1$ kHz), QG-induced or mass-induced delays are close to zero. For a 1 TeV ν , the mass-induced delay is negligible even with $m_\nu = 1$ eV. Taking the expression given in ⁵ as a starting point, neglecting any cosmological effects (for low redshift $z \ll 1$), the delay in ms becomes, in the first order $\Delta t_{\text{QG}}^{\text{ms}} \propto 1/d \simeq 0.15 \left(\frac{E_\nu}{1 \text{ TeV}} \right) \left(\frac{10^{19} \text{ GeV}}{E_{\text{QG}}} \right)$ at 10 kpc, where E_{QG} is the energy scale at which QG effects arise. Taking $E_{\text{QG}} = E_{\text{Planck}} = 10^{19} \text{ GeV}$, this yields a maximum QG delay of 1 second for $E_\nu \approx 1 \text{ TeV}$ and sources as far as the Virgo Cluster ($d \sim 20 \text{ Mpc}$). $\Delta t_{\text{coinc}} = 1 \text{ s}$ thus seems a reasonable choice. The coincidence time window can also be set by imposing an overall coincidence detection probability.

The detection probability for VIRGO can be estimated as a function of the signal-to-ratio (SNR or ρ) of a particular signal, for a given false alarm rate: this is shown for VIRGO in figure 3, for $\rho_{\text{max}} = 5$ (see ^{7,11} for details). In the best case, a threshold corresponding to 1 false alarm every 5 minutes is needed to obtain a 50% detection probability (no beam pattern effects included). The middle panel of figure 3 displays the detection efficiency as a function of ρ_{max} , for this particular false alarm rate, in the case of a single ITF detection or coincident detection in the VIRGO/LIGO network: for low SNRs, the detection by a single ITF is more probable than any twofold coincidence, and the detection by any single ITF is always more efficient than any coincidence configuration ¹¹. In the case of the detection by any of the 3 ITFs, the directional information is not available (no triangulation), and the only relevant information is therefore the *time* of the burst event. Finally, the rms error on the burst arrival time ¹¹ for a gaussian burst of width τ and SNR ρ is $\Delta t^{\text{RMS}} \approx \frac{1.5}{\rho} \left(\frac{\tau}{1 \text{ ms}} \right) \text{ ms}$. This of course limits the accessible QG energy scale, and the coincidence window to be used.

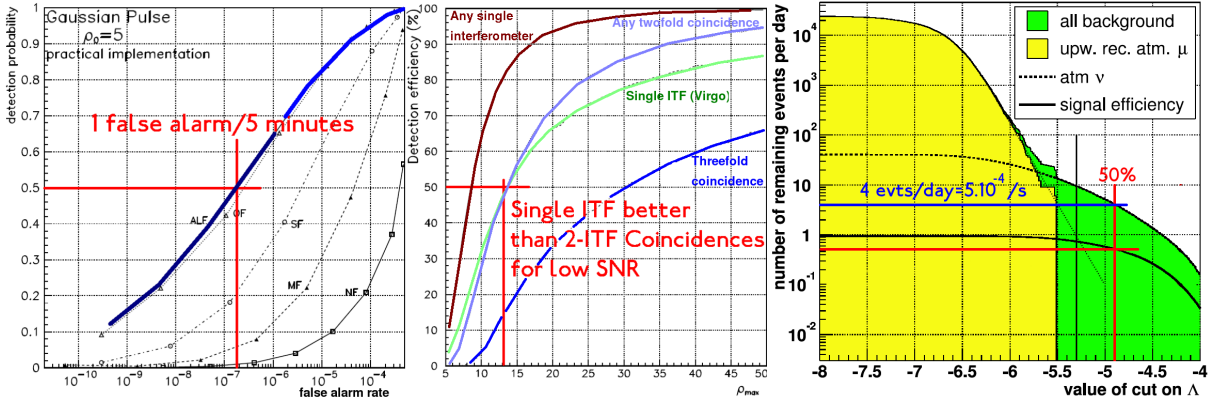


Figure 3: Left : detection probability *vs* false alarm rate, for a $\rho = 5$ gaussian pulse, $\Delta t_{\text{coinc}} = 1 \text{ s}$. Middle : detection probability *vs* ρ_{max} for the different possible detection configurations. Right : Number of background events left as a function of the cut value for Λ . The efficiency for signal is also shown.

In ANTARES, the Čerenkov light emitted by the neutrino-induced muon is detected by an array of photomultipliers arranged in strings, able to reconstruct the energy and direction of the incident muon/neutrino. The quality of the track fit is often expressed in terms of a log-likelihood ratio term which distribution is shown in figure 3, for (upward) atmospheric neutrinos and misreconstructed atmospheric muons, together with the signal detection efficiency for a E^{-2} spectrum. The standard cut applied is $\Lambda = -5.3$, for which the signal efficiency is close to 75% ¹²; the atmospheric ν background is reduced to 10/day.

The plots in figure 3 provide the information needed to estimate the detection probability

$\epsilon_{V,A}$ for a background/false alarm level $R_{V,A}$ in both detectors (V for VIRGO, A for ANTARES). The coincidence detection probability is $\epsilon_{\text{coinc}} = \epsilon_V \epsilon_A$, whereas the coincident accidentals rate in a given time window is $R_{\text{coinc}} = R_V R_A \Delta t_{\text{coinc}}$. Setting $\Delta t_{\text{coinc}} = 1$ s and $R_{\text{coinc}} \sim 1/\text{yr}$, the resulting coincidence detection probability peaks at $\sim 25\%$, for $\Lambda \sim -5.5$. Equivalently, the coincidence detection probability can be set at *e.g.* 50% for a given signal, and the maximal allowed coincidence time window can be extracted. The time coincidence window is maximal for $\epsilon_V \sim 65\%$, reaching ~ 15 ms, for a $\rho = 5$ gaussian burst, with $R_{\text{coinc}} \sim 1/\text{yr}$ ⁷.

4 ANTARES/VIRGO Coincidences

Assuming that both the GW and HE ν signals have been emitted with zero delay at the source, limits can be put on the QG energy scale E_{QG} . Requiring $\epsilon_{\text{coinc}} = 50\%$, the maximum energy scale yielding a measurable effect is limited by GW timing resolution, which depends on the burst duration and SNR, and reaches in this case $E_{\text{QG}}^{\text{max}} \sim 5 \times 10^{18}$ GeV ($\rho = 5$), close to the Planck limit. The minimum accessible energy scale is in turn determined by the maximal coincidence window defined previously, which yields $E_{\text{QG}}^{\text{min}} \sim 10^{17}$ GeV. This is to be compared with existing limits on E_{QG} , *e.g.* using TeV flares from Mrk421 $\sim 4 \times 10^{17}$ GeV¹³. To perform a real *measurement* of E_{QG} , the neutrino energy resolution is of importance, and is a factor 2 or 3 in the case of ANTARES².

VIRGO took data jointly with the 2 LIGO interferometers between May and September 2007, during the *Virgo Scientific Run* (VSR), with a final sensitivity close to the expectation. The interferometer should resume taking data again with an improved injection system in 2009. ANTARES has been continuously taking data with its final 12 line configuration since the end of May 2008, and is expected to observe high energy neutrinos for a period of 10 years. Interestingly, during the *VSR*, ANTARES already had 5 lines operational since January 2007. Clearly, only the most powerful GW/HE ν sources could be detected, but this could be used as a *test bench* for preliminary studies on time coincidences. LIGO data could also be used to enhance the detection probability.

Finally, *circa* 2015, a km³ neutrino telescope should be operating in the Mediterranean Sea¹⁴, along with an ADVANCED VIRGO interferometer¹, with enhanced sensitivity at low frequency: less extremes accretion/ejection scenarios could be probed for microquasars, and interesting constraints on accretion/ejection models could be set by this novel multimessenger approach.

1. VIRGO Collaboration, Class. Quantum Grav. **25** 114045 (2008)
2. Th. Stolarczyk, these proceedings
3. LIGO, Class. Quantum Grav. **25** 114041 (2008); see also [arXiv:0709.0766v2](#)
4. H. Landsman, these proceedings
5. S. Choubey & S. F. King, Phys. Rev. **D67** 073005 (2003)
6. C. Kouveliotou *et al.*, Astrophys.J. **510** L115-118 (1999)
7. Th. Pradier, Proceedings of the VLVT08, 22-24 April 2008, Toulon (France)
8. F. Mirabel, [arXiv:0805.2378v1](#) and references therein
9. For LS5039: F. A. Aharonian *et al.*, J. Phys. Conf. Ser. **39** 408-415 (2006)
10. E. B. Segalis & A. Ori, Phys. Rev. **D64** 064018 (2001)
11. Th. Pradier *et al.*, PRD **63** 042002 (2001); N. Arnaud *et al.*, PRD **65** 042004 (2002)
12. N. Cottini, for ANTARES, these proceedings
13. S. D. Biller *et al.*, Phys. Rev. Lett. **83**, 2108-2111 (1999)
14. K. Lyons, for KM3NET, these proceedings